Journal of Materials Chemistry A

Accepted Manuscript

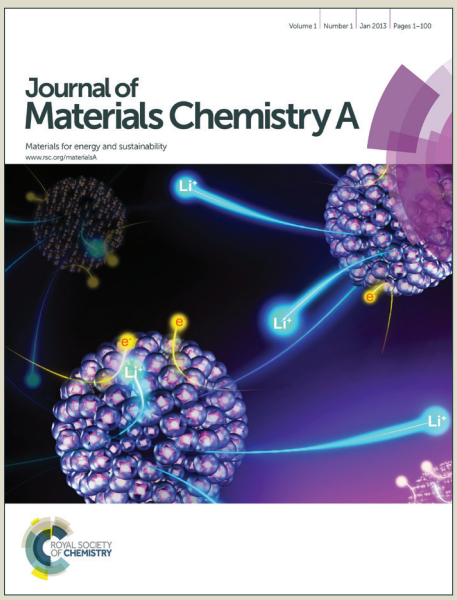

ROYAL SOCIETY OF CHEMISTRY

www.rsc.org/materialsA

Table of Contents

for

Positioning Growth of Scalable Silica Nanorods on the Interior and Exterior Surfaces of Porous Composites

Wenle Li,* Bo Chen and John Y. Walz

A novel yet straightforward one-pot synthesis technique is developed to grow scalable silica nanorods on the interior and exterior surfaces of a porous, inorganic scaffold.

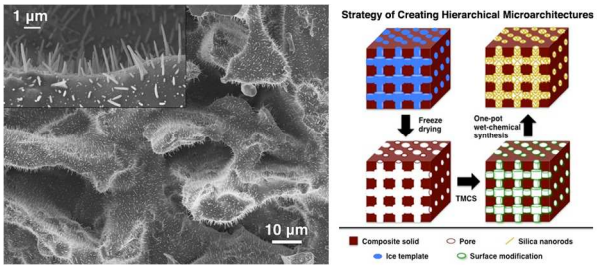

Journal of
Materials Chemistry A

RSCPublishing

ARTICLE

Positioning Growth of Scalable Silica Nanorods on the Interior and Exterior Surfaces of Porous Composites

Cite this: DOI: 10.1039/x0xx00000x

Received 15th September 2014,
Accepted 00th November 2014

DOI: 10.1039/x0xx00000x

www.rsc.org/

Wenle Li,[*,a] Bo Chen[b] and John Y. Walz[c]

A novel yet straightforward one-pot synthesis technique was developed to grow silica nanorods on the interior and exterior surfaces of a porous, inorganic scaffold. Growth of the rods on the surface, versus in the bulk, was achieved by functionalizing the surface with chlorosilane molecules, which allowed the emulsion droplets in which the nanorods grow to anchor to the surface. Rods of 100 – 200 nm diameter and up to 2 μm in length could be grown uniformly over the surface with a typical surface density of 3 rods/μm^2, resulting in an order-of-magnitude increase in the specific surface area (area/mass) of the porous material. It was also shown that the properties of the rods (e.g., size, surface density, shape) could be controlled by changing either the composition of the substrate material or the concentrations of key components in the reacting mixture. Furthermore, by selectively controlling the spatial location of the chlorosilane surface groups, the rods could be grown in specific locations inside the porous material.

Introduction

Hierarchical structures with micro- and/or nano-scale architectures fabricated on three-dimensional networks continue to be of great interest because of their ability to alter the physical and mechanical properties of materials and also introduce additional functionalities. Natural phenomena such as coloration,[1-3] wetting,[4,5] adhesion,[6] and mechanical rigidity[7] strongly depend on this class of structures.[8,9] By combining different length scales into a material, these architectures can also enhance specific macroscopic properties.[10] For example, semiconductor nanowires grown on porous networks improve the performances of solar cells,[10-12] while nanoparticles incorporated inverse opal films display unique optical properties.[2]

Constructing *one-dimensional* micro- and nano-scale architectures (e.g., nanowires[10-13] and nanopillars[5,6,9,14]) into bulk materials not only alters specific surface properties, such as surface area, hydrophobicity, etc., but also provides unidirectional behavior to three-dimensional structures (e.g., electron transport, charge carrier collection).[10] To date, nanowires and nanopillars have been grown on surfaces through vapor–liquid–solid and chemical vapor deposition processes,[10,14] or sculpted on substrates via lithography and ion etching.[9] In spite of the achievements in fabricating controlled microstructures, these techniques can be costly and laborious, especially when targeting large-scale production. Furthermore, many of the reported substructures were developed on either flat surfaces or regular-shaped scaffolds (e.g., nanochannels[10]). By comparison, studies focused on fabricating one-dimensional micro- and nano-scale architectures on arbitrary, multi-dimensional structures are rare due to the complex growing environment.

In this study, we present a straightforward, cost-efficient, and high throughput method for growing silica nanorods on the interior and exterior surfaces of a porous composite with complex geometry. Our strategy was inspired by the wet-chemical synthesis method reported by Kuijk *et al*.[15] Compared to previous synthesis methods,[16] this one-pot approach results in a high yield of particles and makes it possible to create dispersions with high nanorod concentration.[15] Other researchers have used this method to create colloidal particles with a wide variety of shapes, including ribbons, bells and crutches.[17-20] The silica nanorods have been widely adopted in a variety of areas, including information-encoded colloids,[21] permanent dipoles,[22] three-dimensional anisotropic architectures,[23] supracolloidal structures,[24] liquid crystals,[25,26] plastic crystals,[27] and reinforcements for matrix materials.[28]

In each of these prior studies, the rod-like structures were produced in a bulk solution. Here, for the first time, we demonstrate the growth of these nanorods on the *surfaces* of a porous composite material, resulting in a hierarchical structure with greatly enhanced properties.

Synthesis of the silica nanorods was accomplished by hydrolysis and condensation of tetraethyl orthosilicate (TEOS) inside aqueous emulsion droplets. To obtain surface growth of the nanorods, we first functionalized the surface of silica-kaolinite composites with trimethylchlorosilane (TMCS). This functionalization allowed the emulsion droplets to anchor on the composite surface where the nanorod growth occurred, consuming the TEOS contained in the emulsion droplet. Our approach allows tightly controlling a number

of important properties, including rod size, morphology, surface density, and even local position on the substrate. While the work presented here focused solely on silica rods, it is expected that a similar approach could be developed for other inorganic particles, creating hierarchical structures that could be used in such applications as catalysis, sensing and detection, desalination, and drug delivery.[29,30]

Experimental section

Materials

34 wt % silica nanoparticle suspension (Ludox TMA, Sigma-Aldrich, St. Louis, MO), kaolinite powder (Hydrite Flat-D, Imerys Performance Materials, Dry Branch, GA), sodium hydroxide (NaOH, Mallinckrodt, Paris, KY), sodium chloride (NaCl, AR grade, Mallinckrodt, Paris, KY), and deionized water were used to fabricate the various scaffolds used in this study (silica-only, kaolinite-only, and silica-kaolinite composites). The Ludox TMA suspension contained silica particles with nominal diameter of 22 nm and density of 2.37 g/cm^3. Kaolinite particles were disk-like and polydispersed with diameters ranging between 200 nm and 6 μm and thicknesses ranging between 50 and 200 nm.[31] Absolute ethanol, 1-pentanol (≥99%), polyvinylpyrrolidone (PVP, average molecular weight M_n = 40000), sodium citrate dihydrate (99%), ammonia (25 wt% in water), and TEOS were purchased from Sigma-Aldrich and used as-received for the synthesis of nanorods.

Fabrication of porous scaffolds

The freeze-drying and sintering techniques used to fabricate the porous scaffolds were described in prior work.[31,32] In brief, Ludox TMA, kaolinite powder, and NaOH were dispersed/dissolved in water with a total solids loading at 18 vol%. The composite scaffolds used in this study had a kaolinite-to-silica ratio of 5:4. Immediately after the addition of NaCl (concentration maintained at 0.5 M), well-dispersed suspensions were poured into silicone rubber molds where a sol-to-gel transition took place. The samples were then freeze-dried at -35 °C and sintered at 1250 °C.

Surface modification of scaffolds

The porous scaffolds were O_2-plasma cleaned (200 mTorr, 5 min, 100 W) and then exposed immediately to TMCS (99+%, Sigma-Aldrich, St. Louis, MO) vapor overnight, following a previously described procedure.[33]

Growth of silica nanorods on scaffolds

PVP was firstly dissolved in 1-pentanol at a concentration of 0.1 g/mL. After 30 min sonication, the solution was kept overnight to ensure full dissolution. Ethanol, water, and 0.18 M sodium citrate solution at a relative ratio to pentanol of 0.1, 0.028, and 0.01 were then added into the solution in sequence and shaken by hand to form a milky emulsion. A sample of the scaffold (roughly 0.1 cm^3 in volume for each 10 mL pentanol) was then dropped into the emulsion, and the solution was shaken for approximately 5 min. A solution of ammonia and TEOS, each with a relative ratio to pentanol of 0.01 to 0.05, were injected into the emulsion in sequence. The emulsion was shaken after each addition to promote good mixing. The emulsion was then kept overnight (~24 h) with gentle magnetic stirring. Experiments with premature addition of TEOS (i.e., the porous scaffold was added to the solution *after* the addition of TEOS) and also with no magnetic stirring were also conducted to better understand the growth mechanism. After the synthesis, the porous scaffolds were sonicated in ethanol to remove free-standing silica nanorods. The free-standing rod-like particles were also isolated from the emulsion by centrifugation for further characterization.

Preparation of positioning growth sample

After surface modification, a porous scaffold was partially immersed into a fresh piranha solution (i.e., a mixture of sulfuric acid (H_2SO_4, 98 wt%, Spectrum Chemicals & Laboratory Products, Gardena, CA) and hydrogen peroxide (H_2O_2, 30 wt%, Sigma-Aldrich, St. Louis, MO) at ratio of 3:1). After 5 min soaking, the scaffold was lifted out and cleaned with deionized water to remove excess piranha solution. Regions with and without surface groups could be easily distinguished, as the attached TMCS groups alter the hydrophobicity of the substrate.

Characterization of microarchitectures

Microstructures of both scaffolds and free-standing rod-like particles were observed by scanning electron microscopy (SEM, LEO1550, Carl Zeiss MicroImaging Inc., Thornwood, NY). Cross-sections of the porous scaffolds were examined by breaking the samples with a sharp blade. All SEM samples were coated by Au-Pd with an approximate thickness of 5 nm. Nitrogen adsorption-desorption measurements (Autosorb-1 C, Quantachrome Instruments, Boynton Beach, FL) were performed to measure the specific surface area of the porous scaffolds. Elemental analysis was performed by the energy-dispersive X-ray spectroscopy (EDS, Bruker AXS, MiKroanalysis Gmbh, Berlin, Germany) attached to the SEM. The amorphous phase of silica nanorods was identified by transmission electron microscopy (TEM, Philips EM420).

Results and discussion

Our strategy of creating hierarchical microarchitectures (i.e., nanorods on bulk scaffolds) is schematically illustrated in Fig. 1. First, a scaffold with micro-scale porosity was fabricated by freeze-drying and sintering of a kaolinite-silica suspension, following a protocol reported in previous work.[31,32] In this present study, the kaolinite-to-silica ratio in the composite was maintained at 5:4 by volume, and the porosity of the resulting scaffold was previously determined to be ~70%.[34] Since the pores replicated the morphologies of ice crystals that formed during the freezing process, three-dimensional porous structures were produced with typical pore dimensions of tens of microns.

The second step was to functionalize the surfaces of the porous scaffold using TMCS. After cleaning the scaffold with O_2 plasma, the scaffold was immediately exposed to TMCS vapor for an overnight period. This exposure to TMCS was necessary to create Si-O-Si-$(CH_3)_3$ groups on the surface of the scaffold, which are critical for the attachment of the emulsion droplets inside which the silica nanorods grow. The functionalized scaffold was then immersed in a pentanol solution that also contained PVP, ethanol, water, sodium citrate, ammonia, and TEOS and which was the growth solution for the nanorods.

Typical microstructures of the resulting architectures are shown in Fig. 1e. Images were taken from cross-sections of the porous scaffold, which were acquired by breaking the sample with a sharp blade. The insert in the upper left corner of Fig. 1e provides a smaller-scale view of the hierarchical architecture. Nanorods that are 100 - 200 nm diameter and up to 2 μm in length are clearly seen, with a typical surface density of 3 nanorods/μm^2. Nitrogen adsorption measurements show that the nanorods resulted in an order-of-magnitude increase in the specific surface area of the

scaffold (from 6 m^2/g to over 60 m^2/g), while analysis using EDS and TEM showed the nanorods to be amorphous silica.

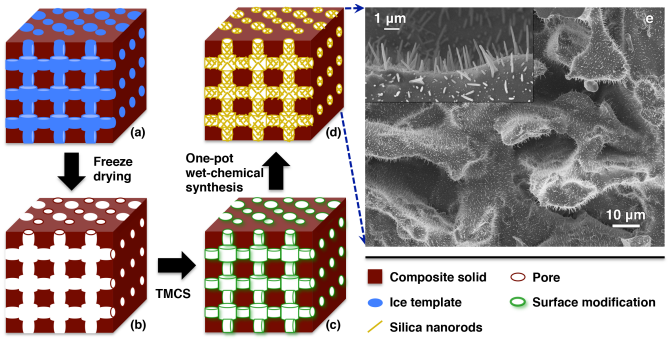

Fig. 1 Growth of silica nanorods on the interior and exterior surfaces of porous composite. Schematic presentation of (a) freezing of kaolinite-silica suspension, (b) porous structure obtained upon sublimation of ice templates, (c) surface modification with TMCS, and (d) growth of silica nanorods through a one-pot wet-chemical synthesis. (e) SEM images showing silica nanorods homogeneously grown on the surfaces of the porous composite.

Growth of the silica nanorods occurs via hydrolysis and condensation of TEOS inside aqueous emulsion droplets. Upon the addition of ethanol, water, and sodium citrate solution to a PVP-pentanol solution, a milky emulsion consisting of dispersed water droplets is obtained (the water-rich emulsion droplets contain a high concentration of PVP[15,19]). The subsequently introduced TEOS rapidly hydrolyzes into a hydrophilic form and dissolves into the water droplets. Condensation of the hydrolyzed TEOS occurs within the droplet and nucleates at the droplet interface. Silica oligomers within the droplet preferably grow onto the existing nuclei, while additional TEOS continuously diffuses into the droplet from the bulk solution. Because the new TEOS can only enter the droplet from the non-nucleus side, one-dimensional growth of silica nanorods is achieved.

Since the growth of the nanorods occurs inside the emulsion droplets, creating surface nanorods requires anchoring the droplets onto the surface prior to initializing the reaction. Our strategy for getting the emulsion droplets to attach to the solid-liquid interfaces is accomplished by creating Si-O-Si-$(CH_3)_3$ groups on the surface via overnight exposure to TMCS vapor. When a water-rich emulsion droplet contacts the surface, these Si-O-Si-$(CH_3)_3$ groups are hydrolyzed and the water drop becomes anchored at the surface. Moreover, these hydrolyzed interfacial oligomers now serve as silica nuclei for the subsequent growth once TEOS is added to the solution (Fig. 2d).

Evidence supporting the attachment of the emulsion droplets onto the scaffold surface is given by the SEM image shown in Fig. 2e. For this image, the synthesis procedure described above was followed except that not TEOS (the silica precursor) was introduced. The scaffold was immersed into the emulsion, removed, gently rinsed, and then air-dried.

Because the emulsion droplets contain a high concentration of PVP, they can be imaged in the dry state.[15] The emulsion droplets, one of which has been identified by an arrow, are clearly visible in Fig. 2e. Note that we hypothesize that the black spots in the image were formed by emulsion droplets that were removed during the rinsing procedure.

Two additional experiments were performed to verify this proposed growth mechanism. In the first experiment, the scaffold, which had been functionalized with the TMCS vapor, was immersed into the emulsion *after* the introduction of TEOS. It was found that while the nanorods grew in the bulk solution, very few nanorods could be found on the surface. This result indicates that having the emulsion droplets anchor on the surface prior to initiating the reaction is a critical step.

The other control experiment involved a comparison test. Two identical syntheses were conducted, however one used stirring of the solution (the normal growth procedure) while one did not. It was found that only with the stirred solution was the homogeneous surface growth achieved (growth of nanorods in the bulk solution does not require stirring). Our hypothesis is that the stirring promotes contact of the emulsion droplet with the functionalized surface.

Fig. 2 summarizes our proposed growth mechanism. The SEM micrographs labeled as a, b, and c were taken from samples in which the growth mechanism was allowed to run for 30 min, 1 h, and 24 h synthesis, respectively. The gradual growth of nanorods from the surface is clear. This one-pot synthesis occurred within 24 h, and no additional growth was detected beyond this time. As can be seen in Fig. 2c, the surface nanorods display a significant variation in length. In addition, the morphology of the nanorods tends to fall into one of two types: one with a tapered, rounded exposed end and a second with a flat exposed end with a diameter that increases away from the surface.

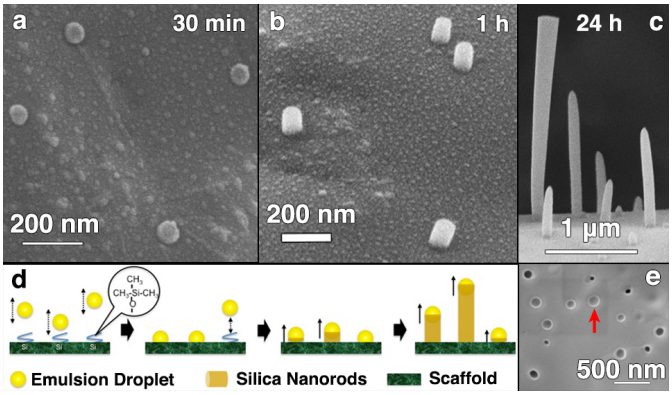

Fig. 2 Mechanism of growth. (a-c) SEM images showing the morphology of silica nanorods grown on the scaffold after 30 min, 1 h, and 24 h, respectively. (d) Schematic for the one-pot wet-chemical growth of silica nanorods on composite scaffold. (e) Emulsion droplets anchored on the interior surface prior to silica precursor addition.

Previous studies revealed that the diameter of the nanorod is determined by the size of the emulsion droplets.[15,19,28] We further speculate that the volume of the nanorod is controlled by the volume of the emulsion droplets. While TEOS can continuously diffuse into the droplet from the bulk during the growth process, the amount of water in each drop is fixed. As a result, the amounts of initial reagents in each emulsion droplet control the resulting dimensions.

In most case, the emulsion droplet gradually shrinks with the consumption of the interior regents, leading to a decrease of the nanorod diameter with growth, which produces the first type of nanorod – tapered with a rounded end. However, if the emulsion droplet detaches from the end of rod-like particle before the exhaustion of regents, the growth ceases, leaving behind a rod with a flat end (i.e., the second type of morphology mentioned above). The cause of the increasing diameter with distance from the surface observed with this type of nanorod morphology is not understood at this point. One possibility is that the contact angle of the droplet on the surface was either significantly different or changed significantly

with growth. Whatever the cause, it should be noted that this second morphology was found in less than 1% of the nanorods observed.

One advantage of this technique is that we can effectively control the dimensions and morphologies of the nanorods. Fig. 3 displays the results of changing three different control parameters – the composition of the surface (i.e., ratio of kaolinite-to-silica used to produce the scaffold), the ammonia concentration, and the TEOS concentration.

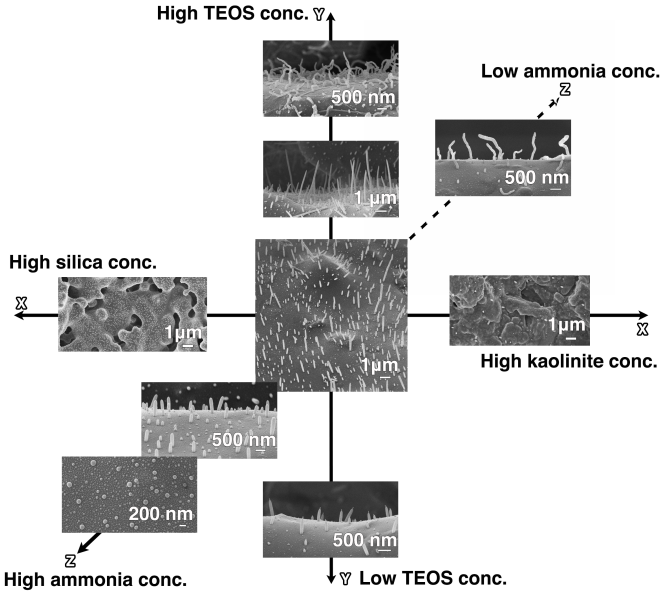

Fig. 3 This schematic illustrate the effects of changing the scaffold composition (*x*-axis), TEOS concentration (*y*-axis) and ammonia concentration (*z*-axis) on the size, density and morphology of the surface nanorods.

In addition to the 5:4 kaolinite-to-silica composites used in the results presented above, we also synthesized nanorods on scaffolds created using only silica and only kaolinite (Fig. 3, *x*-axis). As seen, the nanorods that grew on the composite scaffold (containing both kaolinite and silica) were longer and had a much higher surface density. By comparison, use of the silica-only scaffolds yielded a high density of very short rods (essentially nano 'dots'), while the kaolinite-only scaffolds yielded a much lower density of short rods. At this point, we can only speculate that the very high density on the silica-only scaffolds results from a high concentration of silica surface groups that serve as growth sites, while the kaolinite-only scaffolds present a limited number of such growth sites, explaining the much lower density. It should be mentioned that with both the silica-only and kaolinite-only scaffolds, significant growth of nanorods in the bulk was observed and the dimensions and morphology of these bulk rods were very similar to bulk nanorods that were found to grow with the composite scaffold. We thus conclude that altering the surface chemistry can alter the shape and number of surface nanorods.

The effect of varying the ammonia concentration is presented on the *z*-axis of Fig. 3. The ammonia concentration is an important control parameter as it is reported to influence both the hydrolysis and condensation rates of TEOS.[19] In this study, increasing the ammonia concentration was found to shorten the nanorods, and at high enough ammonia concentration simple hemispheres were observed on the surface. By comparison, decreasing the ammonia concentration produced nanorods that were longer and eventually resulted in the formation of crooked nanorods. One possible explanation for the formation of these crooked nanorods is that the lower ammonia concentration alters the surface tension that maintained the angle between the droplet and the growing direction. It should be mentioned that we observed the same effects (i.e., longer rods that were less straight) on bulk nanorods upon lowering the ammonia concentration.

The final control variable investigated was the TEOS concentration (Fig. 3, *y*-axis). As seen, increasing the concentration of TEOS resulted in longer nanorods with a higher surface density. As the TEOS concentration was increased even further, the rods became crooked, which we again attribute to changes in the surface tension. By contrast, lowering the TEOS concentration resulted in short nanorods at a lower surface density. The result was expected, as the TEOS serves as silica precursor. As with the other control variables studied, the same trends were also observed on rods that grew in the bulk solution.

The experiments described above further demonstrate the possibility of controlling the number density of the surface nanorods. According to the growth mechanism, the surface density of the nanorods is determined by the number of initial emulsion droplets that anchor on the scaffold. Thus increasing either the density of growth sites on the surfaces or the concentration of emulsion droplets in the solution, or alternatively by promoting interactions at the solid-liquid interface, would be expected to result in a higher number density of surface nanorods (Fig. 3). Because the growth of the rod-like particles prefers a relatively static environment (i.e., strong stirring could bend the growing particles), a two-step stirring procedure consisting of initial strong agitation to maximize the number of emulsion droplets, followed by gentle stirring to facilitate nanorod growth, would likely be a good strategy. While optimizing a specific property was beyond the scope of this initial study, a surface density of up to 6 nanorods/μm^2 was achieved. Further improvements in the number density of surface nanorods would be expected to occur through properly designing the scaffold chemistry, ratio of key components, and agitation strategy.

The finding that these surface rods can be created with controlled dimensions and morphologies would clearly be advantageous in developing applications for these materials. One additional finding is that the spatial position of the rods within the scaffold can also be controlled to some degree. As discussed above, the TMCS surface groups are critical in initializing the surface growth of the nanorods, indicating that we can selectively fabricate the nanorods at desired positions within the scaffold. A demonstration of this capability is shown in Fig. 4. In this experiment, a scaffold that had been functionalized with TMCS was partially immersed in a strong acid solution (piranha solution), which was capable of removing the Si-O-Si-$(CH_3)_3$ groups on the surface. This scaffold was then subjected to the same chemical synthesis steps described above. Cross-sections of the resulting structure were then imaged using SEM.

On the scaffold, three regions were identified: no TMCS region, transition region, and TMCS-modified region (Fig. 4). In the TMCS-modified region, nanorods are clearly visible. By contrast, no rod-like particles of any shape or size could be seen in the region that was subjected to the acid etch. Between these two regions is a transition region that was found to contain short nanrods on the surface, which could arise from a capillary action that drew some of the acid solution into the region. While the existence of this transition region indicates that a more sophisticated technique is needed to develop precise spatial patterns within the substrate, these results nonetheless clearly indicate that spatial control of the nanorods within the substrate is possible, which could be highly advantages in specific applications.

The ability to grow scalable silica nanorods on complex architectural scaffolds has numerous potential applications. Perhaps one of the most promising applications, which capitalizes on recent achievements in functionalizing silica surfaces and related hybrid materials, is bio-mimic materials.[35] Our novel design of silica nanorods on ceramic architectures would be beneficial to a new generation of bioceramics, as it facilitates loading of biochemical species that mimic natural systems consisting of cells, signals, and scaffolds.[36]

Furthermore, the dramatic increase in specific surface area would be highly desirable in new types of adsorbents or catalyst materials.[37] Separation membranes with hierarchical structures would be another prospective field. As an example, with silica nanorods grown on one-side of a porous scaffold, a one-piece integrated membrane could be fabricated, reducing the probability of delamination of adjacent layers.[33]

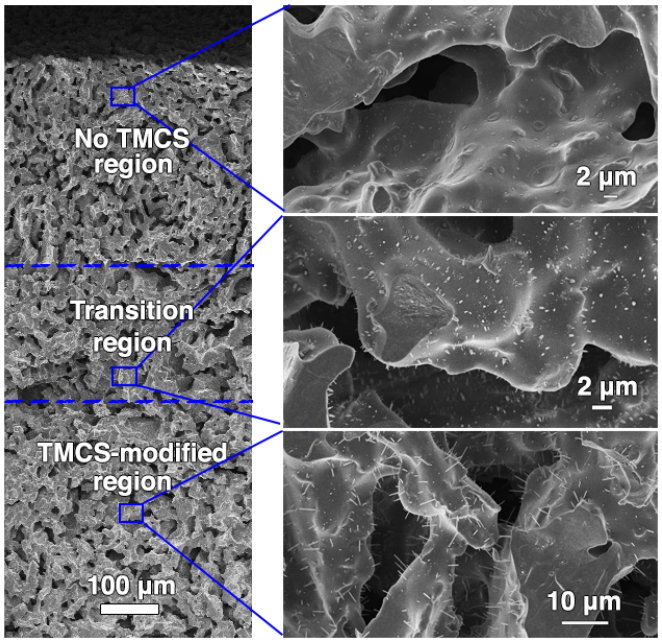

Fig. 4 SEM images showing how nanorods can be grown in a selective area. In the region labeled 'No TMCS', the Si-O-Si-$(CH_3)_3$ surface groups were removed via acid etching.

Conclusions

A straightforward, one-pot synthesis technique was developed that can be used to create silica nanorods on the interior and exterior surfaces of a porous material with complex geometry. Growth of the rods on the surface, versus in the bulk, was achieved by functionalizing the surface with chlorosilane molecules, which allowed the emulsion droplets in which the nanorods grow to anchor to the surface. Rods of 100 – 200 nm diameter and up to 2 µm in length could be grown uniformly over the surface with a typical surface density of 3 rods/µm^2, resulting in an order-of-magnitude increase in the specific surface area of the porous material.

It was also shown that the properties of the rods (i.e., size, surface density, shape) could be controlled by changing either the composition of the substrate material or the concentrations of key components in the reacting mixture. Furthermore, by selectively controlling the spatial location of the chlorosilane surface groups, the rods could be grown in specific locations inside the porous scaffold.

These multi-scale hierarchical materials could find use in a variety of important applications, including catalysis, sensing, molecular separations, and even development of novel biomaterials.[38,39] While these initial studies focused on silica nanorods, which is of great interest because of its optical properties and ease of chemical modification,[15,40] it is expected that similar approaches could also be developed for other inorganic particles, which could open up additional applications.

Acknowledgements

Financial support for this work was provided by the College of Engineering at the University of Kentucky. The work was performed in the Department of Chemical Engineering at Virginia Tech. The authors would like to thank Dr. Abby Whittington for sharing her BET instrument, Dr. Kathy Lu for sharing her freeze dryer, and Dr. Richey Davis for sharing his centrifuge. Assistance from Christopher Winkler at Virginia Tech in TEM analysis is greatly appreciated, as was assistance from the Nanoscale Characterization and Fabrication Laboratory of Virginia Tech.

Notes and references

[a] Department of Chemical Engineering, Virginia Tech, Blacksburg, VA 24061, USA. Email: wenle@vt.edu
Present address:
Department of Materials Science and Engineering, University of Illinois at Urbana-Champaign, Urbana, IL 61801, USA.
The Beckman Institute, University of Illinois at Urbana-Champaign, Urbana, IL 61801, USA.
[b] Center for Energy Harvesting Materials and Systems, Virginia Tech, Blacksburg, VA 24061, USA.
[c] College of Engineering, University of Kentucky, Lexington, KY 40506, USA.

1 P. Vukusic and J. R. Sambles, *Nature*, 2003, **424**, 852.
2 Y. Vasques, M. Kolle, L. Mishchenko, B. D. Hatton and J. Aizenberg, *ACS Photonics*, 2014, **1**, 53.
3 K. R. Phillips, N. Vogel, Y. H. Hu, M. Kolle, C. C. Perry and J. Aizenberg, *Chem. Mater.*, 2014, **26**, 1622.
4 K. H. Chu, R. Xiao and E. N. Wang, *Nat. Mater.*, 2010, **9**, 413.
5 B. D. Hatton and J. Aizenberg, *Nano Lett.*, 2012, **12**, 4551.
6 M. A. Bucaro, Y. Vasquez, B. D. Hatton and J. Aizenberg, *ACS Nano*, 2012, **6**, 6222.
7 J. Aizenberg, J. C. Weaver, M. S. Thanawala, V. C. Sundar, D. E. Morse and P. Fratzl, *Science*, 2005, **309**, 275.
8 W. L. Noorduin, A. Grinthal, L. Mahadevan and J. Aizenberg, *Science*, 2013, **340**, 832.
9 P. Kim, A. K. Epstein, M. Khan, L. D. Zarzar, D. J. Lipomi, G. M. Whitesides and J. Aizenberg, *Nano Lett.*, 2012, **12**, 527.
10 J. Shi, C. L. Sun, M. B. Starr and X. D. Wang, *Nano Lett.*, 2011, **11**, 624.
11 Y. Bai, H. Yu, Z. Li, R. Amal, G. Q. Lu and L. Z. Wang, *Adv. Mater.*, 2012, **24**, 5850.

12 M. Law, L. E. Greene, J. C. Johnson, R. Saykally and P. D. Yang, *Nat. Mater.*, 2005, **4**, 455.
13 J. Shi and X. D. Wang, *Energ. Environ. Sci.*, 2012, **5**, 7918.
14 Z. Y. Fan, H. Razavi, J. W. Do, A. Moriwaki, O. Ergen, Y. L. Chueh, P. W. Leu, J. C. Ho, T. Takahashi, L. A. Reichertz, S. Neale, K. Yu, M. Wu, J. W. Ager and A. Javey, *Nat. Mater.*, 2009, **8**, 648.
15 A. Kuijk, A. van Blaaderen and A. Imhof, *J. Am. Chem. Soc.*, 2011, **133**, 2346.
16 C. M. van Kats, P. M. Johnson, J. E. A. M. van den Meerakker and A. van Blaaderen, *Langmuir*, 2004, **20**, 11201.
17 P. Datskos, J. Chen and J. Sharma, *RSC Adv.*, 2014, **4**, 2291.
18 P. Datskos and J. Sharma, *Angew. Chem. Int. Edit.*, 2014, **53**, 451.
19 A. Q. Zhang, H. J. Li, D. J. Qian and M. Chen, *Nanotechnology*, 2014, **25**, 135608.
20 J. He, B. Y. Yu, M. J. Hourwitz, Y. J. Liu, M. T. Perez, J. Yang and Z. H. Nie, *Angew. Chem. Int. Edit.*, 2012, **51**, 3268.
21 K. Chaudhary, Q. Chen, J. J. Juarez, S. Granick and J. A. Lewis, *J. Am. Chem. Soc.*, 2012, **134**, 12901.
22 J. Yan, K. Chaudhary, S. C. Bae and J. A. Lewis, *Nat. Commun.*, 2013, **4**, 1516.
23 M. Fu, K. Chaudhary, J. G. Lange, H. S. Kim, J. J. Juarez, J. A. Lewis and P. V. Braun, *Adv. Mater.*, 2014, **26**, 1740.
24 K. Chaudhary, J. J. Juarez, Q. Chen, S. Granick and J. A. Lewis, *Soft Matter*, 2014, **10**, 1320.
25 T. Xu and V. A. Davis, *Langmuir*, 2014, **30**, 4806.
26 G. J. Vroege, *Liq. Cryst.*, 2014, **41**,342.
27 B. Liu, T. H. Besseling, M. Hermes, A. F. Demirors, A. Imhof and A. van Blaaderen, *Nat. Commun.*, 2014, **5**, 3092.
28 W. Li, K. Lu, J. Y. Walz and M. Anderson, *J. Am. Ceram. Soc.*, 2013, **96**, 398.
29 H. R. Vutukuri, J. Stiefelhagen, T. Vissers, A. Imhof and A. van Blaaderen, *Adv. Mater.*, 2012, **24**, 412.
30 M. Mullner, T. Lunkenbein, J. Breu, F. Caruso and A. H. E. Muller, *Chem. Mater.*, 2012, **24**, 1802.
31 W. Li, K. Lu and J. Y. Walz, *J. Am. Ceram. Soc.*, 2011, **94**, 1256.
32 W. Li, K. Lu and J. Y. Walz, *J. Am. Ceram. Soc.*, 2012, **95**, 883.
33 W. Li and J. Y. Walz, *Sci. Rep.*, 2014, **4**, 4418.
34 W. Li, K. Lu and J. Y. Walz, *J. Mater. Sci.*, 2012, **47**, 6882.
35 M. Vallet-Regí, M. Colilla, B. González, *Chem. Soc. Rev.*, 2011, **40**, 596.
36 L. G. Griffith, G. Naughton, *Science*, 2002, **295**, 1009.
37 D. Xia, T. Cheng, W. Xiao, K. Liu, Z. Wang, G. Liu, H. Li, W. Wang, *ChemCatChem*, 2013, **5**, 1784.
38 A. Sidorenko, T. Krupenkin, A. Taylor, P. Fratzl and J. Aizenberg, *Science*, 2007, **315**, 487.
39 Y. Vasquez, E. M. Fenton, V. F. Chernow and J. Aizenberg, *CrystEngComm*, 2011, **13**, 1077.
40 N. Hijnen and P. S. Clegg, *Chem. Mater.*, 2012, **24**, 3449.

